J. Hydrol. Hydromech., 73, 2025, 2, 175–189
https://doi.org/10.2478/johh-2025-0013

sciendo Journal of Hydrology and Hydromechanics Institute of Hydrology SAS

Clear water scour at eco-friendly wood-based structures in vegetated channels

Deep Roy[1], Simone Pagliara[2*], Michele Palermo[3]

[1] Department of Civil Engineering, Indian Institute of Engineering Science and Technology, Shibpur, Howrah, West Bengal 711103, India.
[2] Laboratory of Hydraulics, Hydrology and Glaciology (VAW), ETH Zurich, Zurich 8093, Switzerland.
[3] DESTEC-Department of Energy, Systems, Territory and Construction Engineering, University of Pisa, Via Gabba 22, Pisa 56122, Italy.
[*] Corresponding author. E-mail: pagliara@vaw.baug.ethz.ch

Abstract: Worked Wood Piles (WWP) belong to the category of low-head eco-friendly restoration structures made from large woody debris that are often placed in the vicinity of riverbanks to realign the flow towards the central part of the channel, thereby stabilizing river embankment. Moreover, significant growth of in-stream vegetation usually occurs in the downstream wake region of WWPs, affecting the scour and dune morphology formed around such structures crucial for promoting biodiversity. To model these phenomena, we conducted experiments under clear water condition with isolated and multiple WWPs in series in the presence and absence of in-stream vegetation in horizontal channels under a large range of hydraulic, structural and vegetation configurations. The results captured the effect of growing stages of in-stream natural vegetation on the scour process in correspondence with WWPs. It was observed that inflow conditions and structure geometry greatly affect the equilibrium scour morphology whereas the number and height of vegetation impacts the maximum scour and dune lengths. In addition, different scour morphology types were distinguished and their fields of existence were established based on flow, structure and vegetation parameters. Finally, we derived empirical equations allowing practitioners to quantify the maximum scour depth and length as well as the dune height.

Keywords: Hydraulics; Scour; Vegetation; Worked Wood Pile (WWP).

1 INTRODUCTION

Rivers are a key component of many ecosystems. Most of them are more and more threatened by anthropogenic activities, leading to an overall degradation in terms of stability, sediment-carrying potential, and biodiversity. Generally, the construction of dams and weirs alters the natural hydrological regimes (Bayley, 1991), while the channel straightening and shortening, as well as the clearing of woody debris and vegetation leads to habitats degradation (Gippel, 1995). Such anthropogenic modifications to the river flow regime and channel leads to rupture of both longitudinal and lateral connectivity across the river basin resulting in decrease in fish diversity (Stoffers, et al., 2022). A viable solution to this problem is offered by the implementation of various rock and wood-based in-stream low-head structures resulting in deep scour holes in the downstream stilling basin which act as biodiversity hotspots and allow better fish migration (Kurdistani, et al., 2023). For example, Scurlock et al. (2012a, 2012b) studied the scour morphologies due to A-, U-, and W-shaped rock weirs installed in straight channels. Also, short grade-control structures like block ramps were studied extensively in straight and curved channels which helps in energy dissipation (Pagliara, et al., 2008; Palermo, et al., 2021). Among such structure types, an active option for restoring riverine systems is represented by wood-based structures constructed from Large Wood (LW) logs, which aim at modifying the sediment-carrying potential of rivers as well as at enhancing biodiversity. LW logs are characterized by a diameter greater than 0.1 m and a length greater than 1 m (Keller and Swanson, 1979). These can lead to complex riverbed morphologies of alternating scours and dunes, influencing the formation of habitat features (Fischenich and Morrow, 2000). Even though LW accumulation at hydraulic structures may lead to increased flood levels (Schalko et al., 2018, 2020) and pronounced scour formations threatening structure stability, an optimum quantity is essential as a source of fine particulate organic matter, as well as an active agent to stabilize channel dimensions and to promote aquatic ecosystem (Pagliara et al., 2020a).

In the past, woody debris have been extensively used as component of several low-head eco-friendly structures (Maryland Department of the Environment Water Management Administration, 2000). Submerged vanes have been often used to control sediment load and to prevent excessive erosion of the outer bank of meandering rivers (Odgaard and Spoljaric, 1986; Odgaard and Mosconi, 1987; Bhuiyan et al., 2010). Among wood-based structures, the hydraulic behaviour and scour characteristics due to different types of log-vanes and log-deflectors were investigated by Pagliara et al. (2015, 2020a) and Pagliara and Kurdistani (2016), also providing key design guidelines for such structures. These are particularly useful for riverbank protection and for enhancing biodiversity in the freshwater system. Neuhaus and Mende (2021) provided a practical perspective on the application of Engineered Large Wood Structures (LWS) in field scenarios including challenges involved in benchmarking appropriate LW quantities. Pagliara et al. (2021) analyzed the morphological features due to wood bundles made of LW, whose main applicability is to deflect high velocity flows away from the riverbank and to create suitable resting pools for fish migration. Low-head LW-based structures are often associated with the growth of in-stream vegetation, particularly, on the sand banks formed in the low flow season. This vegetation offers a significant resistance to flow and results in alterations in the flow regime and bed morphology of the channel (Kałuża, et al., 2018). Although, the flow interaction and turbulent structures within in-stream vegetation patches has been studied by researchers (Jahadi et al., 2019), there is a crucial gap in knowledge regarding the effect of growing stages of in-stream natural vegetation on the scour process in correspondence with low-head LW based hydraulic structures. In addition, the temporal evolution of the planar extent of the scour and dune formations due to low-head structures is an important consideration from design perspective which has not been studied rigorously in previous studies. To fill this gap in literature, Roy and Pagliara (2022a) designed a novel LW based low-head eco-friendly structure named Worked Wood Piles (WWPs) and provided a preliminary analysis on the temporal and equilibrium scour morphologies in unvegetated channels. The current study aims to extend the analysis of WWP to straight vegetated channels. Novel experimental tests were conducted with isolated and multiple WWPs in series in presence of in-stream vegetation in the downstream stilling basin. The main goals of this research are: (i) to characterise the temporal and equilibrium scour morphology due to WWPs in clear water condition; (ii) to provide empirical equations capable to predict the main riverbed morphological characteristics due to WWPs (i.e., maximum scour depth and dune height, and maximum scour length); (iii) to assess the effect of growing stages of in-stream natural vegetation on the scour parameters in correspondence with WWP structures.

2 MATERIALS AND METHODS

2.1 Experimental setup

Experiments with WWPs were carried out at the hydraulics laboratory of the University of Pisa, following the same methodology and with identical structure configuration as that reported in Roy and Pagliara (2022a). Tests were conducted in a straight horizontal flume, which was 11 m long, 0.5 m wide (B) and 0.5 m deep. A uniform bed material was used to simulate the mobile bed, with d_{50} = 1 mm and $\sigma = (d_{84}/d_{16})^{0.5} = 1.15$ and ρ_s = 2467 kg/m^3, where d_{xx} is the material size for which xx% of the material is finer, σ is the non-uniformity coefficient and ρ_s is the bed material density. Such bed diameter sizes are typically used to model scour phenomena at hydraulic structures in real rivers (Pagliara et al., 2017). Before setting up a test, the mobile channel bed was ensured to have a horizontal surface. Thereafter, the target discharge was slowly set up and the tailwater level was controlled and kept constant throughout a test using a sluice gate located at the downstream end of the channel. All tests were conducted under clear water conditions (Oliveto and Hager, 2002), with $0.79 \leq U/U_c \leq 0.86$, where U and U_c are the mean velocity and mean threshold velocity calculated according to Neill (1968). After each test, the channel was dried, and the resulting equilibrium scour morphology was surveyed with a “Leica Geosystems” laser scanner. The recorded data cloud was processed using the ‘Cyclone’ software to generate scour maps of the entire stilling basin with an accuracy of ±1 mm. In addition, a 0.1 mm precise point gauge was employed to measure water depths as well as principal scour and dune features and this data was used to cross validate the precision of the laser scanner generated scour maps (see also Roy and Pagliara, 2022b; Roy et al., 2021).

Tests were conducted with different structure configurations, i.e., isolated and multiple (2 or 3) WWPs in series under identical hydraulic conditions. Consequently, the number of structures n ranged between 1 and 3. For $2 \leq n \leq 3$, the distance d between two consecutive WWPs was chosen in such a way that $d/B = 0.6$. To ensure fully developed flow conditions, the first WWP was placed at $s/B = 15.8$, with s denoting the distance between the channel entrance and the structure (Wilkerson, et al., 2019). A single WWP was made of three vertical primary trunks of wood (diameter = 0.015 m), linked together with the help of metallic strings (Keller and Swanson, 1979). The height of the structure above the original bed level is denoted by h_{st} and for the current study $h_{st}/B = 0.17$. Horizontal wood branches (diameter = 0.002 – 0.003 m, total length = 0.1 m) were used to reinforce the trunks. Some of the branches were aligned with the flow direction, others at a 60° angle with respect to the flow. All tests were conducted for $b/B = 0.2$, with b representing the maximum transverse width (and the longitudinal length) of a single WWP. (Note that b/B is also the maximum diameter of the circumference encompassing the structure and represents the maximum transversal blockage width of an individual WWP in the direction perpendicular to the flow). Notably, the horizontal branches were located at two distinct depths from the top of the structure, i.e., at $0.25h_{st}$ and $0.75h_{st}$. Below the bed level, the primary trunks were attached to solid foundation to keep the arrangement upright during test. Note that the foundation did not interfere with the scour process, as it was located much deeper compared to the maximum scour depth reached in the present study.

To provide sidewall protection against scour, a longitudinal wooden member (diameter = 0.015 m) was introduced along the channel wall. The length of the wooden member is denoted by l_p, with l_p/B = 0.6, 1.2 and 1.8 for n equal to 1, 2 and 3, respectively. The top surface of the wooden member coincided with the original bed level.

Figure 1 shows the stilling basin for $n = 2$ in the presence of vegetation along with major hydraulic and scour parameters. Namely, the maximum scour depth is denoted by z_m and mostly occurs in the vicinity of the first structure. There are deep scour holes formed separately in the vicinity of each WWP structure in series. However, these scour holes are connected by shallower scour contours and the longitudinal maximum scour length of the entire scour zone is denoted by l_m (Figure 1). Similarly, z_M and l_M represent the maximum height and the longitudinal extension of dune formations, respectively. Notably, the dune region is generally discontinuous due to the presence of consecutive WWP structures and scour holes. Furthermore, the flow discharge is denoted by Q whereas the tailwater depth is denoted by h_{tw}.

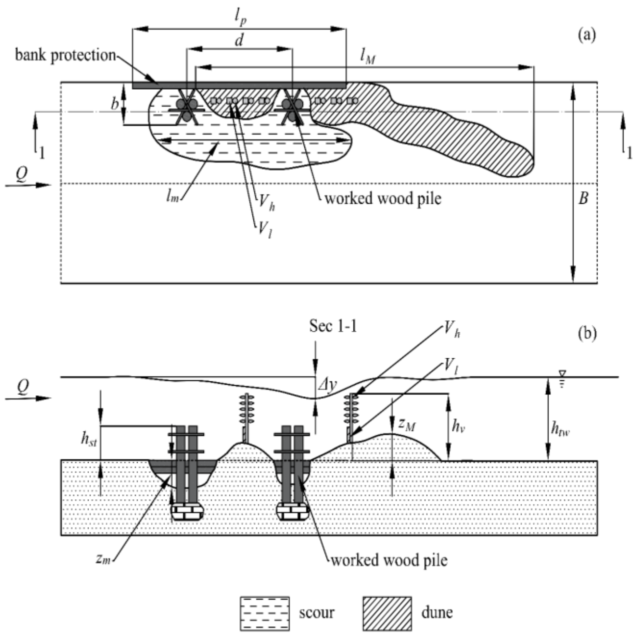

Fig. 1. Schematic diagram sketch of the experimental apparatus with the indication of the main hydraulic and scour parameters: a) plan and b) side views.

Two types of vegetation were inserted in the WWPs stilling basin. The first type is characterised by low height shrub vegetation which bears resemblance to the initial stage of vegetation growth downstream of hydraulic structures and is denoted by V_l (see Figure 2a). In the above-mentioned case, individual vegetation elements have a planar cross-sectional area of 1 cm^2 and h_v = 0.045 m where h_v is the height of vegetation element. The second type, termed V_h, is characterised by high leafy vegetation which simulates the fully grown phase of vegetation in the stilling basin (see Figure 2b). This type is characterised by a planar cross-sectional area of 1 cm^2 and h_v = 0.09 m.

Tests were conducted as follows. First, reference tests (phase 0, termed A_0) were carried out for 4 hours with both isolated and multiple WWPs (n = 2 or 3) in series in unvegetated channels under identical hydraulic conditions (Note that preliminary longer tests—up to 8 hours—were also conducted, revealing average differences in scour depth of approximately 5% between 2 and 8 hours, thus indicating a quasi-equilibrium condition for practical applications corroborated by Melville and Chiew, 1999). Then, tests were repeated under identical hydraulic conditions and were characterized by three phases (termed A_1, A_2 and A_3), reflecting different stages of the natural process of growth of vegetation.

Namely, in the phase A_1, each test was conducted with isolated or multiple WWPs (n = 2 or 3) in series in an unvegetated channel. The duration of this phase was t_1 = 2 hours, with t_i indicating the duration of the phase A_i and i is an integer ranging from 1 to 3. Subsequently, the flow was stopped, and the scour morphology was surveyed. Then, in the second phase (A_2), a predetermined number of vegetation elements (n_v) belonging to type V_l was placed in the region between consecutive WWPs and in the downstream stilling basin in various formations (symmetric and staggered) and on the dune area formed during the phase A_1. The number of individual vegetation elements (n_v) varied as well, depending on the extension of the dune formations. This resembled the early stage of growth of in-stream vegetation on sand bars in natural rivers during low flow periods. The test was re-started, and its duration was t_2 = 1 hour. Following this, the flow was stopped again, and the scour morphology was surveyed. In the third phase (A_3), each individual vegetation element of V_l was bundled together with an additional vegetation element belonging to type V_h, thus maintaining the same spatial formation of phase A_2 (Figure 1b). This arrangement resembles fully grown stage of in-stream vegetation. Then the test was re-started and lasted t_3 = 1 hour. Note that the overall duration of the three phases was $t_t = t_1 + t_2 + t_3$ = 4 hours, allowing us to directly compare resulting equilibrium morphology with that of the corresponding reference test A_0, characterized by the same duration. A summary of the experimental data has been provided in Table 1 (Appendices). It is worth remarking that, for the tested range of parameters, the Reynolds number (Re) varied between 34965 to 81395 which mostly resulted in rough, turbulent flow regime in the channel. On the other hand, the Froude number (F) of the incoming flow varied between 0.31 to 0.46, similar to values observed in natural channels. Therefore, considering a natural channel having width less than 20 m, the model scale can be assumed to be greater than 1:40. According to Heller (2011), the scale effects become negligible under such flow conditions. Figures 2c and d show the equilibrium scour morphology due to experimental test pertaining to phase A_3 in presence of two WWPs in series formation and an isolated WWP, respectively, with downstream vegetation.

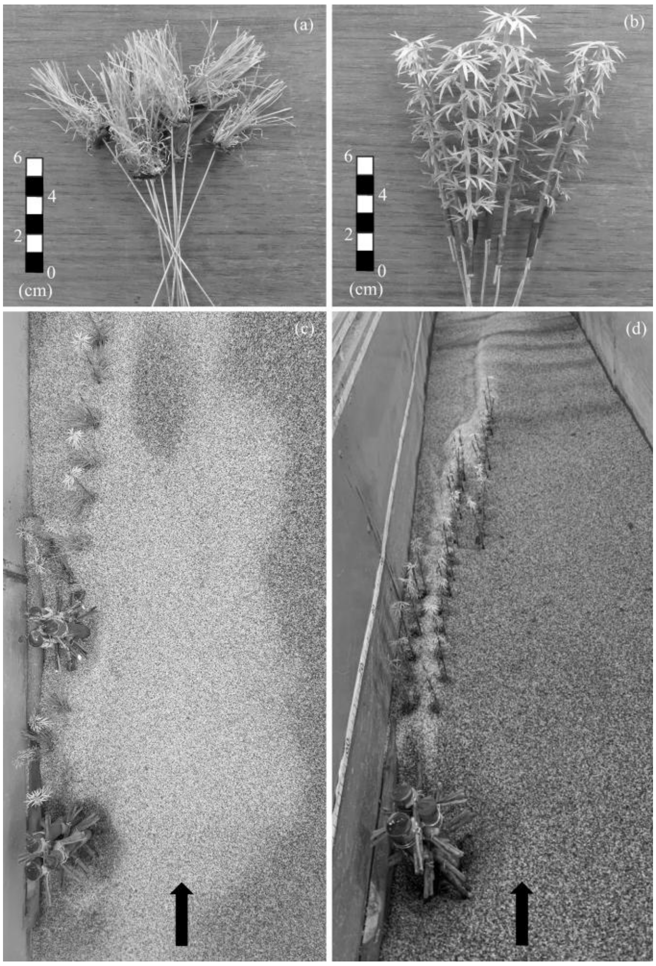

Fig. 2. Vegetation type a) V_l and b) V_h; equilibrium scour morphology pertaining to experimental test with c) two WWPs in series formation and d) an isolated WWP at the end of phase A_3 (the black arrows in c and d indicate the direction of flow).

2.2 Dimensional analysis

A detailed dimensional analysis was conducted to identify the governing non-dimensional groups influencing the scour process (Barenblatt, 1987). Following the theoretical approach proposed by Bombardelli, et al. (2018) and experimental evidence by Palermo et al. (2020), a characteristic length φ of the scour and dune geometry can be expressed as function of the following parameters:

$$\varphi = f(Q, h_{st}, b, h_{tw}, B, d, n, g, \Delta\rho, \rho, d_{50}, h_v, n_v, t) \quad (1)$$

In the above equation, g denotes the acceleration due to gravity, $\Delta\rho = \rho_s - \rho$ is the reduced density, with ρ indicating the water density, and t is the time from the beginning of phase A_1 to the end of phase A_3 (i.e., $0 \leq t \leq t_1$, $t_1 < t \leq t_1 + t_2$, and $t_1 + t_2 < t \leq t_t$ for phases A_1, A_2 and A_3, respectively). Furthermore, according to Dey and Raikar (2005), Dey and Sarkar (2006) and (2008), the variable $\Delta\rho$ should be preferred to ρ_s in scour processes. Therefore, by applying the Buckingham-Π theorem and the incomplete self-similarity theory (Barenblatt, 1987), with Q, h_{tw} and ρ as the repeating variables, and after re-arranging some non-dimensional groups, the following functional relationship can be derived (Pagliara et al., 2020b; Roy and Pagliara, 2022b):

$$\Phi = f\left(\frac{h_{st}}{h_{tw}}, \frac{b}{B}, \frac{B}{h_{st}}, \frac{d}{B}, n, \mathrm{F}_{d50}, \frac{\Delta\rho}{\rho}, \frac{d_{50}}{B}, \frac{h_v}{h_{tw}}, n_v, \frac{t}{T}\right) \quad (2)$$

where Φ is the non-dimensional characteristic length and F_{d50} represents the densimetric Froude number:

$$F_{d50} = \frac{Q}{Bh_{tw}\sqrt{gd_{50}(\Delta\rho/\rho)}} \tag{3}$$

Note that the densimetric Froude number combines the effects of flow parameters and bed sediment characteristics and is similar to other parameters typically used for other scour problems at low-head structures (D'Agostino and Ferro, 2004; Palermo et al., 2021). Moreover, the group t/T appearing in Eq. (2) represents the non-dimensional time, and the reference time T can be expressed as:

$$T = \frac{b}{\sqrt{gd_{50}(\Delta\rho/\rho)}} \tag{4}$$

Note that T is the same reference time adopted by Di Nardi, et al. (2021) and (2022), who applied a theoretical approach based on the phenomenological theory of turbulence to different scour phenomena, under both steady and unsteady flow conditions. The range of variation of the governing non-dimensional groups in Eq. (2) are as follows: $0.90 \le h_{st}/h_{tw} \le 2.36$, $b/B = 0.2$, $B/h_{st} = 5.88$, $d/B = 0.6$, $1 \le n \le 3$, $2.31 \le F_{d50} \le 2.48$, $\Delta\rho/\rho = 1.467$, $d_{50}/B = 0.002$, $0 \le h_v/h_{tw} \le 2.5$, $0 \le n_v \le 31$ and $2.39 \le t/T \le 4.79$ (corresponding to $t_1/T \le t/T \le t_t/T$, since the evolution was analyzed from the end of phase A_1 to the end of phase A_3).

3 RESULTS AND DISCUSSION

3.1 Maximum scour depth and dune height

One of the most important characteristic lengths is the maximum scour depth z_m, or equivalently the diffusion length z_m+h_{tw} (Hoffmans and Verheij, 1997; Bombardelli et al., 2018; Di Nardi, et al., 2021 and 2022). Following the dimensional analysis carried out in the preceding section, and assuming $\varphi = z_m+h_{tw}$, we derived the non-dimensional, dependent variable $\Phi = (z_m+h_{tw})/B$ accounting for maximum scour depth. Considering that some of the independent governing groups b/B, B/h_{st}, d/B, $\Delta\rho/\rho$ and d_{50}/B have been kept constant, Eq. (2) can be rewritten as follows:

$$\Phi = \frac{(z_m+h_{tw})}{B} = f\left(\frac{h_{st}}{h_{tw}}, n, F_{d50}, \frac{h_v}{h_{tw}}, n_v, \frac{t}{T}\right) \tag{5}$$

To analyze the trend of maximum scour depth data, Figures 3a-d contrast experimental values of $(z_m+h_{tw})/B$ against F_{d50} for reference tests A_0, and phases A_1, A_2 and A_3. The data trend is essentially identical in all four cases, thus corroborating that the maximum scour depth is basically at quasi-equilibrium at the end of phase A_1, i.e., for $t_1 = 2$ hours. Namely, the scour depth does not significantly vary for $t > t_1$, and it is very close to that obtained at the end of phases A_2, A_3 and corresponding reference test A_0. Notably, V_l type vegetation was placed in the downstream stilling basin of the WWP during phase A_2 (duration $t_2 = 1$ hour) and subsequently additional V_h type vegetation was placed in the stilling basin during phase A_3 (duration $t_3 = 1$ hour). Within the tested range of parameters, the presence of vegetation parameters did not cause significant local erosion, i.e., it did not affect the dependent variable $(z_m+h_{tw})/B$. In other words, the maximum scour depth attained at $t_1 = 2$ hours was maintained throughout phases A_2 and A_3 without any significant increment. However, it is worth mentioning, that although maximum scour depth becomes almost constant at $t = t_1$, the presence of vegetation alters the flow conditions, resulting in planar modifications of the scour hole and dune up to $t = t_t$ (i.e., at the end of phase A_3. See also Roy and Pagliara, 2022a). Therefore, considering that t/T, h_v/h_{tw} and n_v do not affect $(z_m+h_{tw})/B$ in the tested range of parameters, Eq. (5) can be rewritten as:

$$\frac{(z_m+h_{tw})}{B} = f\left(\frac{h_{st}}{h_{tw}}, n, F_{d50}\right) \tag{6}$$

A further consideration is in order. The effective blockage area in case of isolated WWP or that of multiple WWPs in series depends on n and h_{tw} in case of unsubmerged structures ($h_{st} > h_{tw}$). Conversely, in case of submerged structure ($h_{st} < h_{tw}$), it is dependent on n and h_{st}. Moreover, although the maximum scour depth always occurs in the vicinity of the first structure in case of WWP series, the number of structures in series formation (n) slightly affects $(z_m+h_{tw})/B$.

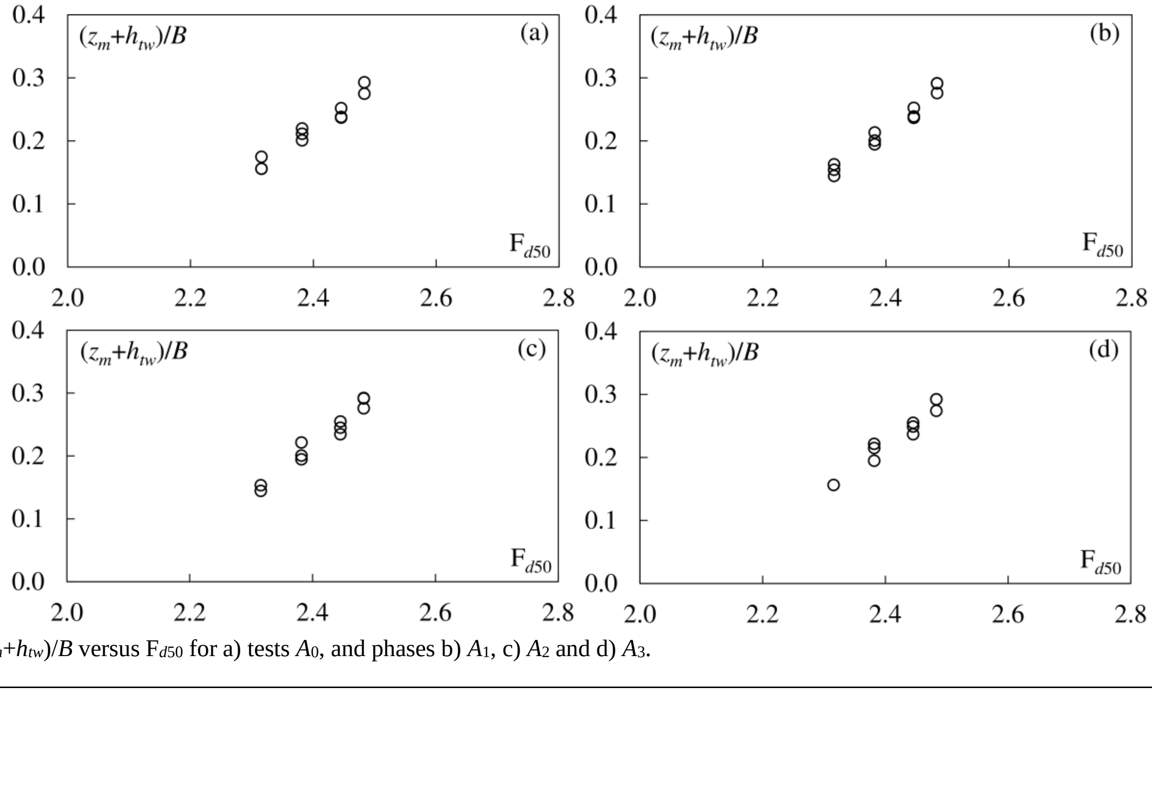

Fig. 3. $(z_m+h_{tw})/B$ versus F_{d50} for a) tests A_0, and phases b) A_1, c) A_2 and d) A_3.

Therefore, an equivalent densimetric Froude number, consistent with the physics of scour formation at WWP, has been derived as follows:

$$\mathrm{F}_{deq} = \mathrm{F}_{d50}\left[n\frac{min(h_{tw},h_{st})}{h_{tw}}\right]^{-0.0086} \quad (7)$$

valid for $2.31 \le \mathrm{F}_{d50} \le 2.48$, $0.90 \le h_{st}/h_{tw} \le 2.36$ and $1 \le n \le 3$. Notably, the introduction of the equivalent densimetric Froude number F_{deq} allowed us to consider the effects of all governing non-dimensional parameters using a unique variable. Therefore, Eq. (6) can be further modified as follows:

$$\frac{(z_m+h_{tw})}{B} = f\left(\mathrm{F}_{deq}\right) \quad (8)$$

It is worth mentioning that, according to Bombardelli et al. (2018), Bormann and Julien (1991) and Hoffmans (1998), the diffusion length (z_m+h_{tw}) increases with the flow power in the channel and decreases with the particle diameter, i.e., it increases with F_{d50}. Conversely, the variable h_{st}/h_{tw} accounts for the effect of the relative submergence of the structure which does not depend on the diffusion length, but on the structure height and tailwater depth.

The data corresponding to $(z_m+h_{tw})/B$ has been replotted against F_{deq} for both reference tests A_0, and phases A_1, A_2 and A_3 (Figures 4a, b, c and d, respectively), corroborating that $(z_m+h_{tw})/B$ only depends on F_{deq}. Consequently, the following Eq. (9) was derived, and it successfully predicts values of $(z_m+h_{tw})/B$ pertaining to all reference tests and different phases (see Figure 5).

$$\frac{(z_m+h_{tw})}{B} = 0.000065exp(3.39\mathrm{F}_{deq}) \quad (9)$$

Equation 9 is valid for $2.29 \le \mathrm{F}_{deq} \le 2.48$, $0.90 \le h_{st}/h_{tw} \le 2.36$, $1 \le n \le 3$, $b/B = 0.2$, $B/h_{st} = 5.88$, $d/B = 0.6$, $\Delta\rho/\rho = 1.467$, $d_{50}/B = 0.002$, $0 \le h_v/h_{tw} \le 2.5$, $0 \le n_v \le 31$ and $2.39 \le t/T \le 4.79$. Also Eq. (9) is applicable for $0.79 \le U/U_c \le 0.86$ corresponding to clear water condition. It is worth remarking that Eq. (9) can predict the maximum scour depth at isolated and multiple WWPs in series both in vegetated and unvegetated straight channels with a high level of accuracy (R^2 = 0.98) and will provide a viable tool for practitioners to facilitate the design of WWP and its downstream stilling basin. Moreover, Eq. (9) has the same analytical form as the general class of empirical formulae used for scour prediction at various low-head hydraulic structures like block ramps, double winged log frames, wood bundles etc (Pagliara et al., 2020a, b).

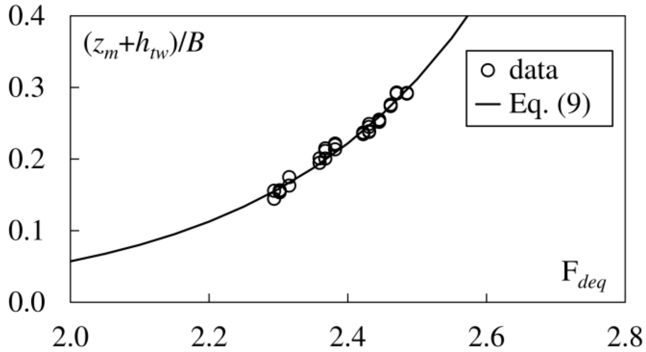

Fig. 5. $(z_m+h_{tw})/B$ versus F_{deq} for all phases and reference tests.

The maximum dune height (z_M) occurring in correspondence with isolated or multiple WWPs in series represents another important parameter. It is worth remarking that the formation of a dune along the channel bank limits the development of the scour hole, and, consequently, the increase of the scour depth (see also Pagliara et al., 2006). This leads to enhanced protection against failure by excessive scour for the WWP foundation and channel banks. Also, dunes provide spawning sites for fishes. Experimental data pertaining to dune height were analyzed following the same methodology adopted for the maximum scour depth. Experimental evidence suggests that z_M also attains maximum value at the end of the phase A_1 (i.e., at $t = t_1$) showing coherence with the trend in case of maximum scour depth.

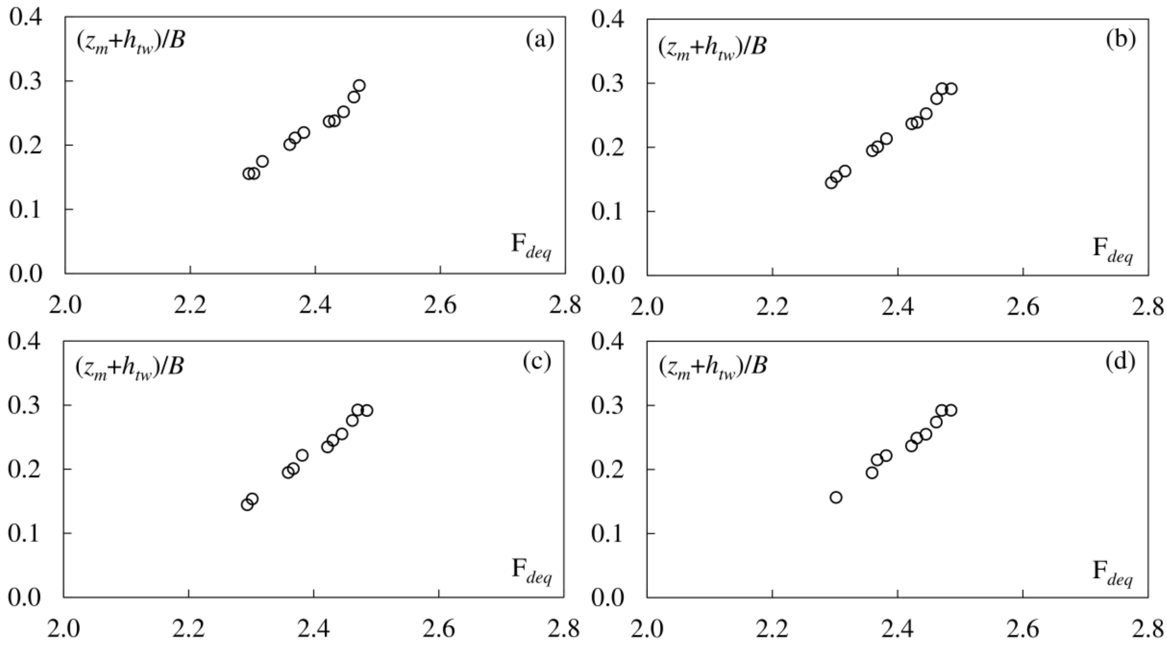

Fig. 4. $(z_m+h_{tw})/B$ versus F_{deq} for a) reference tests A_0, and phases b) A_1, c) A_2 and d) A_3.

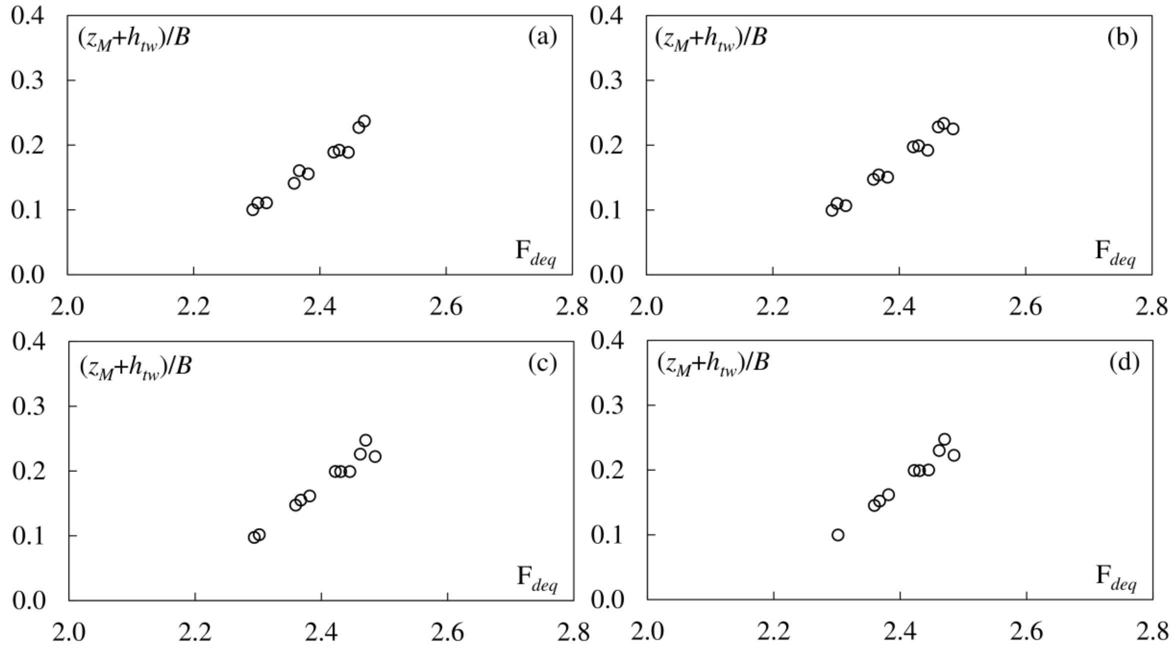

Fig. 6. $(z_M+h_{tw})/B$ versus F_{deq} for a) reference tests A_0, and phases b) A_1, c) A_2 and d) A_3.

Considering that vegetation is introduced in the channel at $t = t_1$ (i.e., at the beginning of phase A_2), the previous observation implies that vegetation parameters (h_v/h_{tw}, n_v) also do not affect the dependent variable $\Phi = (z_M + h_{tw})/B$ within the tested range of parameters. Such observations are further evidenced in Figure 6 where $(z_M+h_{tw})/B$ values are contrasted against corresponding values of F_{deq} for reference tests as well as tests with various growing stages of in-stream vegetation. Therefore, the following empirical equation has been derived:

$$\frac{(z_M+h_{tw})}{B} = 0.000003 exp(4.55F_{deq}) \quad (10)$$

Eq. (10) is valid for $2.29 \le F_{deq} \le 2.48$, $0.90 \le h_{st}/h_{tw} \le 2.36$, $1 \le n \le 3$, $b/B = 0.2$, $B/h_{st} = 5.88$, $d/B = 0.6$, $\Delta\rho/\rho = 1.467$, $d_{50}/B = 0.002$, $0 \le h_v/h_{tw} \le 2.5$, $0 \le n_v \le 31$ and $2.39 \le t/T \le 4.79$. Also, Eq. (10) is applicable for $0.79 \le U/U_c \le 0.86$ corresponding to clear water condition. Notably Eq. (10) predicts the data trend quite well ($R^2 = 0.95$) and can be used to estimate the maximum dune height for isolated WWP and WWP series in unvegetated as well as vegetated horizontal channels within the tested range of parameters (Figure 7).

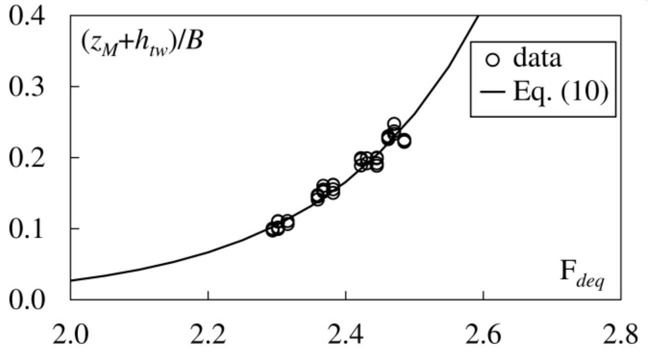

Fig. 7. $(z_M+h_{tw})/B$ versus F_{deq} for all tests, both in presence and absence of vegetation.

3.2 Maximum scour hole and dune length

The maximum longitudinal scour and dune lengths, i.e., l_m and l_M, respectively, are important features to characterize the scour pothole and dune regions at equilibrium. Unlike maximum scour depth and dune height, experimental observations suggest that both l_m and l_M values continue to increase for $t > t_1$ hours and reaches their equilibrium value at $t = 4$ hours (i.e., at $t = t_t$, or, equivalently, at the end of phase A_3 and reference test). In other words, after 2 hours, the scour hole and the dune extend longitudinally without varying their depth and height, respectively. This occurrence implies that, unlike other scour phenomena (e.g., jet driven scour processes), the scour hole does not evolve homothetically (for further details, see Bombardelli et al., 2018). Consequently, l_m and l_M are affected by the presence of vegetation downstream of WWP and depends on h_v/h_{tw} and n_v. Based on these observations and the dimensional analysis, from Eq. (5) it follows that the dependent parameter $(l_m+h_{tw})/B$ is function of:

$$\frac{(l_m+h_{tw})}{B} = f\left(\frac{h_{st}}{h_{tw}}, n, F_{d50}, \frac{h_v}{h_{tw}}, n_v, \frac{t}{T}\right) \quad (11)$$

By introducing F_{deq}, the above equation can be further simplified as follows:

$$\frac{(l_m+h_{tw})}{B} = f\left(F_{deq}, \frac{h_v}{h_{tw}}, n_v, \frac{t}{T}\right) \quad (12)$$

The analysis was conducted by steps. Firstly, the values of $(l_m+h_{tw})/B$ at $t = t_1$ (i.e., at the end of phase A_1) and at equilibrium for reference tests (i.e., at $t = t_t$) were compared in order to quantify the effect of the non-dimensional time parameter t/T. Note that for phase A_1 and reference tests, the channel is unvegetated, consequently Eq. (12) becomes:

$$\frac{(l_m+h_{tw})}{B} = f\left(F_{deq}, \frac{t}{T}\right) \quad (13)$$

By contrasting experimental values of $(l_m+h_{tw})/B$ against F_{deq} (Figure 8a), it can be observed that data points corresponding to reference tests A_0 show considerably higher values than those pertaining to phase A_1. Differently from other scour phenomena (for further details, see Di Nardi et al., 2021 and 2022), this occurrence and findings shown in Figure 3 corroborate that scour process does not evolve homothetically for these structures, i.e., the ratio z_m/l_m depends on the time t. Namely, the analysis of data allowed us to establish that $(l_m+h_{tw})/B$ can be expressed as only function of the combined parameter $F_{deq}(t/T)^{0.2}$, accounting for the time evolution of scour length in the absence of vegetation, with t ranging from t_1 to t_t (Figure 8b). Thereby using $F_{deq}(t/T)^{0.2}$ as independent non-dimensional parameter, the following predicting equation was derived:

$$\frac{(l_m+h_{tw})}{B} = 0.0145exp\left[1.40F_{deq}\left(\frac{t}{T}\right)^{0.2}\right] \qquad (14)$$

The above equation is valid in absence of downstream vegetation for the following range of tested parameters: $2.29 \le F_{deq} \le 2.48$, $0.90 \le h_{st}/h_{tw} \le 2.36$, $1 \le n \le 3$, $b/B = 0.2$, $B/h_{st} = 5.88$, $d/B = 0.6$, $\Delta\rho/\rho = 1.467$, $d_{50}/B = 0.002$, and $2.39 \le t/T \le 4.79$. Also, Eq. (14) is applicable for the range $0.79 \le U/U_c \le 0.86$ which corresponds to clear water condition. Moreover, Eq. (14) predicts the data trend with sufficient accuracy ($R^2 = 0.75$, Figure 8c). It is worth mentioning that scour and dune length values are generally much greater than scour depth and dune height (Breusers and Raudkivi, 1991; Hoffmans and Verheij, 1997). Moreover Eq. (14) differs from Eq. (9) since it contains the non-dimensional time t/T. As also evidenced by other authors, experimental measurements of scour length are generally affected by larger uncertainties compared to those of scour depth, resulting in a bigger data dispersion which explains the reduction of R^2 in Eq. (14). Thereafter, we extended the analysis to the maximum scour length due to single WWP and WWP series in presence of vegetation (phase A_2 and A_3). In this case, $(l_m+h_{tw})/B$ can be expressed by the non-dimensional functional relationship shown in Eq. (12). Following the same analysis as that of the previous case in unvegetated channels, experimental values of $(l_m+h_{tw})/B$ were classified according to the different phases (i.e., phase A_2 with low vegetation V_l and phase A_3 with high vegetation V_h) and contrasted against the non-dimensional parameter $F_{deq}(t/T)^{0.2}$ in Figure 9a. Overall, data pertaining to phase A_3 are characterized by higher values of both the independent and dependent variables, i.e., $F_{deq}(t/T)^{0.2}$ and $(l_m+h_{tw})/B$, respectively, thus corroborating the effect of vegetation on the scour length evolution from phase A_2 to phase A_3. Such effect is further highlighted in Figure 9b, where experimental values of $(l_m+h_{tw})/B$ are classified into two groups according to the number of individual vegetation elements in a test (n_v) and plotted against $F_{deq}(t/T)^{0.2}$. It can be observed that $(l_m+h_{tw})/B$ generally increases with n_v within the tested range of parameters. From a physical point of view, in case of emergent vegetation (i.e., for $h_v > h_{tw}$), the blockage ratio depends on both n_v and h_{tw}; conversely, for submerged vegetation (i.e., for $h_v < h_{tw}$), the blockage depends on n_v and h_v. All such effects can be accounted for by introducing the parameter F_{vdeq} calculated as follows:

$$F_{vdeq} = F_{deq}\left(\frac{t}{T}\right)^{0.2}\left[1 + n_v\frac{min(h_{tw},h_v)}{h_{tw}}\right] \qquad (15)$$

The above equations is valid for $2.29 \le F_{deq} \le 2.48$, $0.47 \le h_v/h_{tw} \le 2.5$, $7 \le n_v \le 31$ and $3.59 \le t/T \le 4.79$. In fact, F_{vdeq} accounts for all the parameters influencing the temporal evolution of the scour length for vegetated channels.

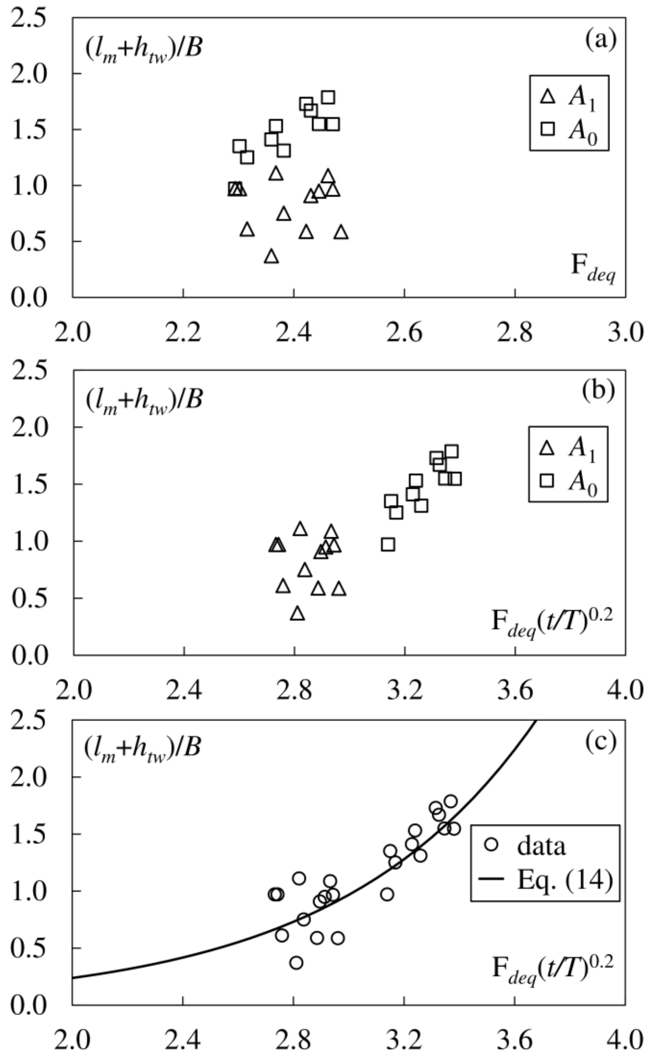

Fig. 8. $(l_m+h_{tw})/B$ versus a) F_{deq}, b) $F_{deq}(t/T)^{0.2}$; c) Plot of Eq. (14) along with experimental data pertaining to phase A_1 and reference tests A_0.

Furthermore, it is worth remarking that $F_{vdeq} = F_{deq}(t/T)^{0.2}$ for unvegetated channels (i.e., for $n_v = 0$; $h_v/h_{tw} = 0$), which is consistent with the physics of the phenomenon. Consequently, using F_{vdeq}, Eq. (12) can be further simplified as follows:

$$\frac{(l_m+h_{tw})}{B} = f\left(F_{vdeq}\right) \qquad (16)$$

Figure 9c shows the plot of $(l_m+h_{tw})/B$ vs F_{vdeq} with data grouped according to the phases A_2 and A_3, corroborating that F_{vdeq} is a suitable parameter to represent the physics of the phenomenon, since a unique trend for all data can now be identified. Therefore, by interpolating experimental data in vegetated channels, the following empirical relations could be derived:

$$\frac{(l_m+h_{tw})}{B} = 0.48ln\left(F_{vdeq}\right) - 0.24 \qquad (17)$$

The above equation is valid for $2.29 \le F_{deq} \le 2.48$, $0.90 \le h_{st}/h_{tw} \le 2.36$, $1 \le n \le 3$, $b/B = 0.2$, $B/h_{st} = 5.88$, $d/B = 0.6$, $\Delta\rho/\rho = 1.467$, $d_{50}/B = 0.002$, $0.47 \le h_v/h_{tw} \le 2.5$, $7 \le n_v \le 31$ and $3.59 \le t/T \le 4.79$. In addition, Eq. (17) is applicable for $0.79 \le U/U_c \le 0.86$ corresponding to clear water condition. Note that Eq. (17) predicts the maximum scour length in the presence of downstream vegetation for both single WWP and WWPs series in straight channels with a sufficient degree of accuracy (R^2 = 0.77, Figure 9d). In addition, by comparing Figures 8c and 9d pertaining to unvegetated and vegetated channels, respectively, it can be observed that the presence of vegetation modifies the kinetics of scour hole evolution, that is analytically reflected in the change from exponential to logarithmic trend in Eqs. (14) and (17), respectively.

The maximum axial dune length was analyzed using the same non-dimensional framework as other scour parameters where $\Phi = (l_M+h_{tw})/B$. However, unlike that in case of maximum scour length, $(l_M+h_{tw})/B$ data shows significant scatter when plotted against $\mathrm{F}_{deq}(t/T)^{0.2}/\mathrm{F}_{vdeq}$ which did not allow to derive a predicting equation. Nonetheless, some considerations can be done about the physics of the phenomenon. In case of unvegetated channels (reference tests A_0 and phase A_1), $(l_M+h_{tw})/B$ values have been contrasted against $\mathrm{F}_{deq}(t/T)^{0.2}$ and classified according to the number of structures in the WWP series arrangement (n). On the other hand, for vegetated channels (phase A_2 and A_3), $(l_M+h_{tw})/B$ values have been contrasted against F_{vdeq} and classified according to n. Experimental evidence confirm that $(l_M+h_{tw})/B$ usually increases with n for both unvegetated (reference tests A_0 and phase A_1, Figure 10a) and vegetated channels (phase A_2 and A_3, Figure 10b).

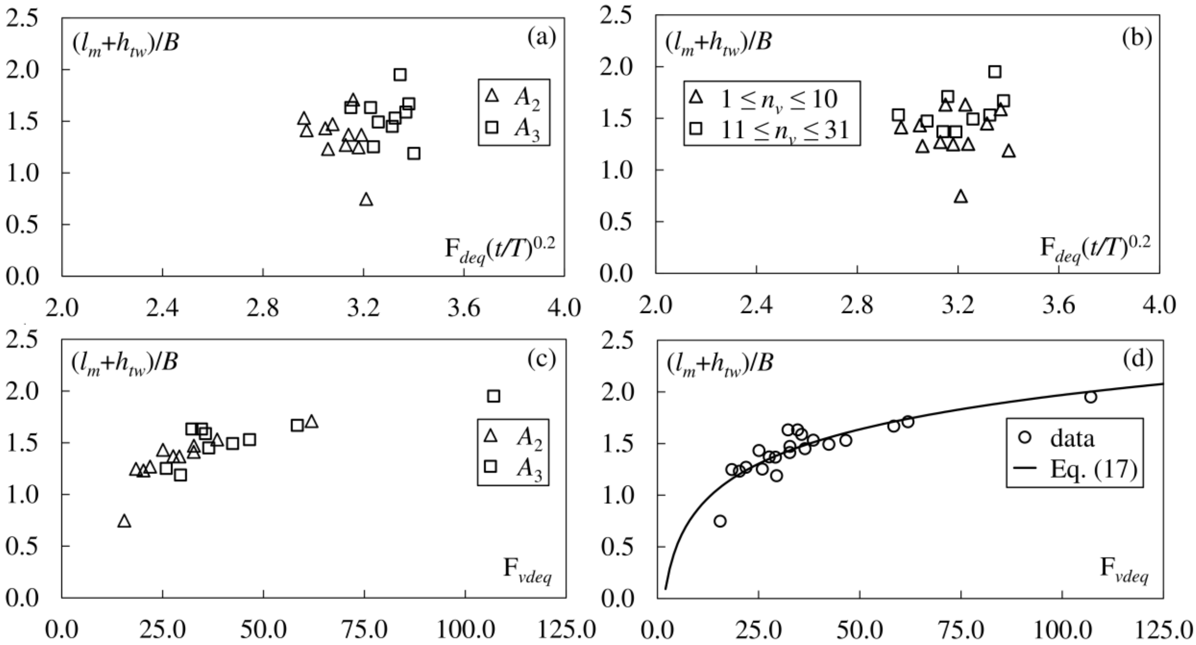

Fig. 9. $(l_m+h_{tw})/B$ versus $\mathrm{F}_{deq}(t/T)^{0.2}$ with data grouped according to a) different phases (A_2 and A_3) and b) n_v. $(l_m+h_{tw})/B$ versus F_{vdeq} c) with data grouped according to different phases (A_2 and A_3) and d) along with the plot of Eq. (17).

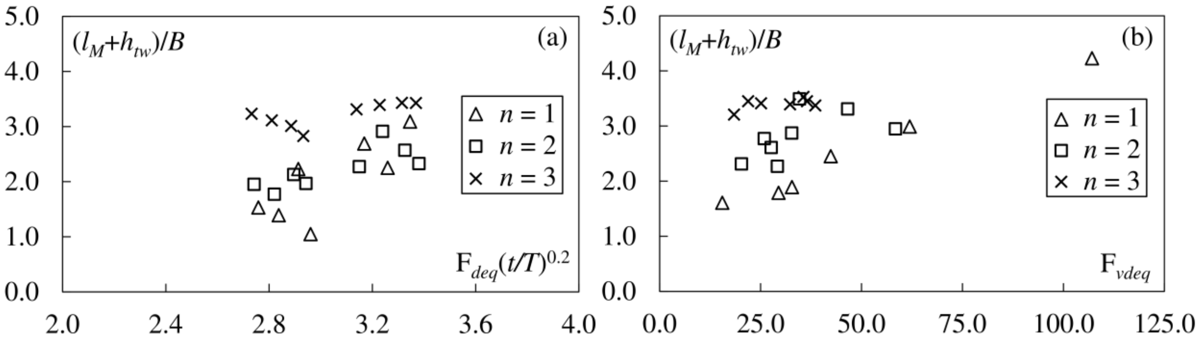

Fig. 10. a) $(l_M+h_{tw})/B$ versus $\mathrm{F}_{deq}(t/T)^{0.2}$ for reference tests A_0 and phase A_1; b) $(l_M+h_{tw})/B$ versus.

3.3 Scour features

From a design perspective, the investigation of the equilibrium morphology due to WWPs under a range of hydraulic and structural conditions is of paramount importance. Likewise, the temporal evolution of scour and dune geometries is equally important for design purposes, as flood events may not be long enough to allow the equilibrium conditions to be established. For such implications, the morphological features at various stages of time were also investigated. Figure 11 presents temporal scour evolution maps at selected times (i.e., for t = 10, 30, 60, 120, and 240 minutes) for isolated (n = 1) and series of two (n = 2) WWPs, flow discharges ranging between $0.008 \le Q \le 0.014$ m^3/s, tailwater depths $0.056 \le h_{tw} \le 0.094$ m, $0.79 \le U/U_c \le 0.86$ and $0.90 \le h_{st}/h_{tw} \le 1.52$. For an isolated WWP (Figures 11a), the scour hole starts evolving from the beginning of the test and elongates towards downstream until reaching equilibrium configuration after approximately 240 min. Contemporarily, the dune starts forming just downstream of the WWP, then stretches steadily along the channel bank, resembling a wing-like formation. For this structure configuration, both the scour and dune planar area enlarge at a uniform rate with time till they eventually reach a quasi-equilibrium configuration. The dynamics of the evolution does not vary for $n = 1$ in the tested range of hydraulic conditions (Figure 11b).

In case of a series of two WWPs ($n = 2$), initially, different scour holes form around each structure. Then, at a later stage, they combine resulting in a unique, elongated shape extending downstream (Figure 11c). In contrast to the case $n = 1$, the scour hole enlargement rate is initially slower (in the first 60 min), then it rapidly increases until the equilibrium condition is reached at $t = 240$ min. Dune formations develop in the region between the structures as well as in the downstream stilling basin. Namely, dunes enlarge at a uniform rate in the first stage of the evolution, covering the area between the two WWPs for $t \leq 30$ min. Furthermore, the dune downstream of the second structure grows resembling a wing-like formation, resulting in a rapid elongation for $t > 30$ – 60 minutes that confines the scour in the central part of the channel. The increase of both Q and h_{tw} leads to an overall similar temporal evolution of the bed morphology (Figure 11d), with more pronounced dune and scour formations for comparable t. A further increase of Q and h_{tw} (Figure 11e and f) results in scours featuring small circular shapes around the WWPs for $t < 10$ min, then rapidly enlarging with time and resembling the characteristic elongated shape highlighted before. The dune formations follow the same pattern discussed before (Figure 11c, d). Therefore, unlike to the single WWP case ($n = 1$), the inflow conditions significantly influence the scour and dune formation rates for multiple WWPs arranged in series configuration.

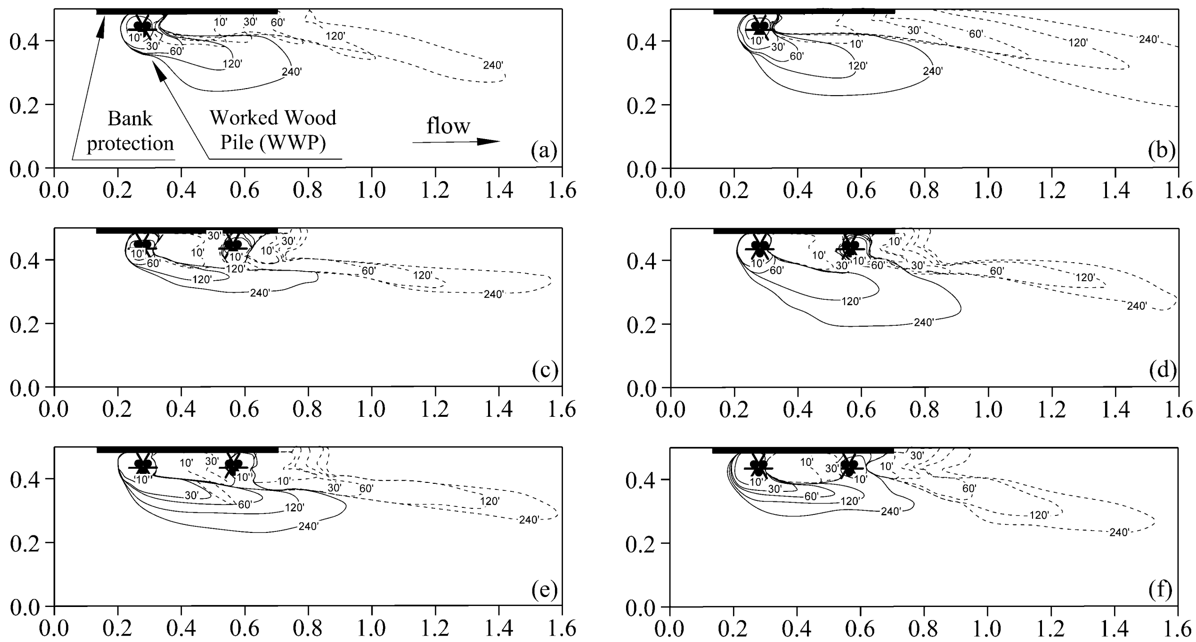

Fig. 11. Temporal evolution of scour hole and dune for test: (a) 5, (b) 4, (c) 17, (d) 21, (e) 22, and (f) 26. Filled lines refer to scour, dashed lines to dune. Axis dimensions are in meters.

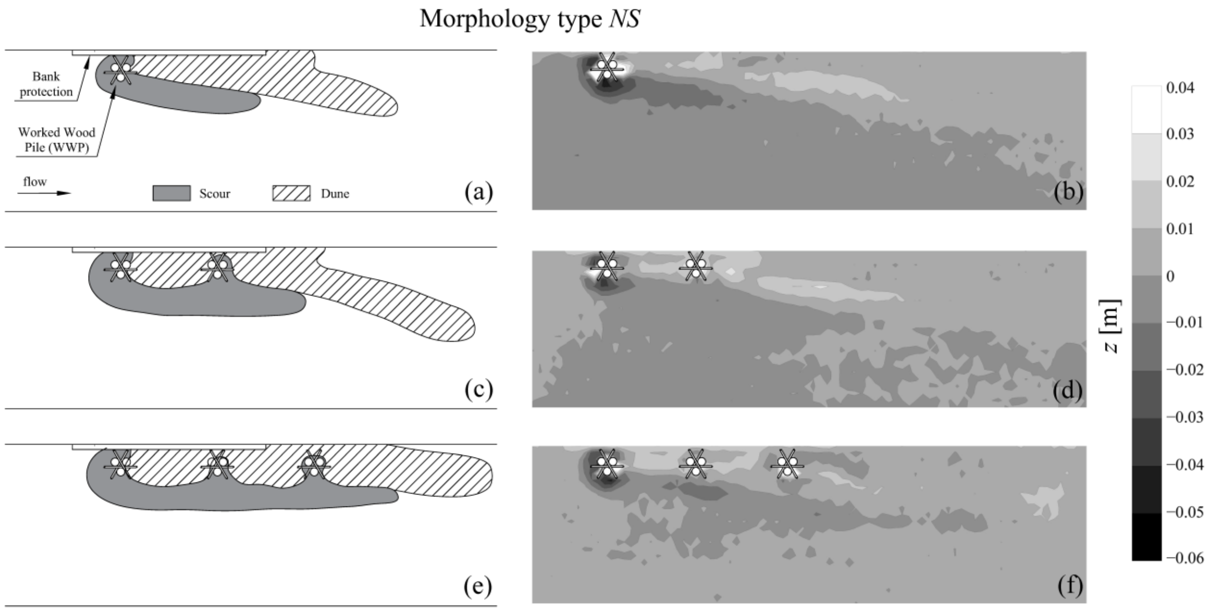

Fig. 12. Conceptual sketches of morphology type *NS* (No Scour) for n equal to (a) 1, (c) 2, and (e) 3; contour maps for tests (b) 5, (d) 22, and (f) 41.

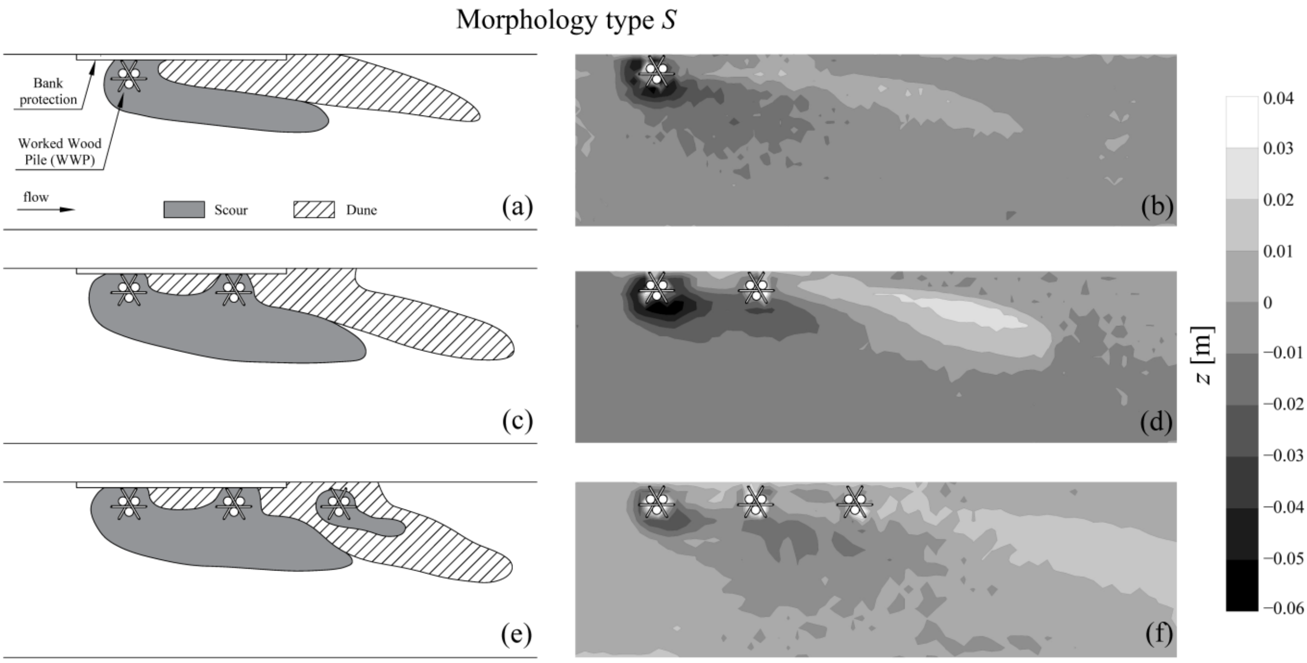

Fig. 13. Conceptual sketches of morphology type *S* (Scour) for *n* equal to (a) 1, (c) 2, and (e) 3; contour maps for tests (b) 12, (d) 17, and (f) 30.

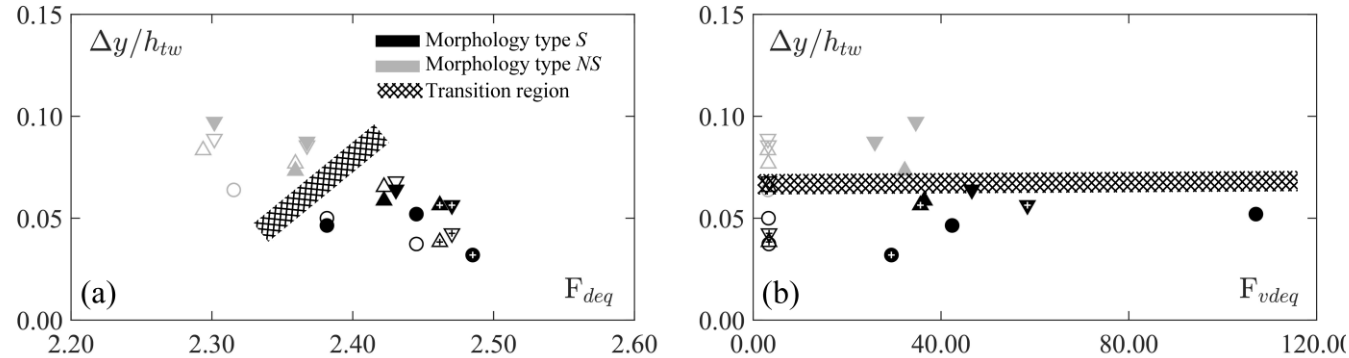

Fig. 14. Existence fields of the scour morphology types *S* and *NS* for WWPs: (a) $\Delta y/h_{tw}$ versus F_{deq}; (b) $\Delta y/h_{tw}$ versus F_{vdeq}. Circles refer to $n = 1$, up-pointing triangle to $n = 2$, down-pointing triangle to $n = 3$; filled symbols refer to tests with presence of vegetation, empty symbols to tests with no vegetation; plus-signs refer to tests with submerged WWPs.

The knowledge of the qualitative scour morphology types is fundamental for a correct design of such structures and to properly determine sites for dredge disposal and aquatic species refuge, as well as to identify areas of the channel bank prone to excessive erosion and thus in need of proper protection. To this end, equilibrium scour morphologies pertaining to phase A_3 (with vegetation) and reference tests A_0 (without vegetation) were classified. Namely, two morphology types were identified, i.e., type *NS* ("No Scour") and type *S* ("Scour"). The morphology type *NS* (Figure 12) is characterized by the absence of scour downstream of the isolated WWP or downstream of the first structure in a series arrangement, a very shallow scour around the WWPs, and a pronounced and elongated dune formation directly connected to the downstream end of the first structure. For series configurations ($n = 2$ in Figure 12c, d; $n = 3$ in Figure 12e, f), an additional, significant dune forms in between of the structures, confining the scour towards the centre of the channel, thus avoiding excessive erosion around the additional structures in series arrangement. This results in natural bank protection enhancement, as well as non-excessive scour formation around the WWPs.

The morphology type *S* (Figure 13) is characterized by a pronounced scour all around the isolated WWP (or the first structure in case of series arrangement), and by a dune formation shifted downstream compared to the *NS*-type, thus not connected to the first WWP. For series configurations ($n = 2$ in Figure 13c, d; $n = 3$ in Figure 13e, f), the dune formation is less extended compared to the *NS*-type, leading to lower scour confinement and thus to more pronounced scour forming around the WWPs. This in turn results in a significant scour around the isolated WWP (or the first structure in series arrangement), promoting erosion of the channel bank. Therefore, additional bank protection should be carefully designed for morphology types *S*. Moreover, in both the above cases, the scour potholes in conjugation with extended dune bars downstream of the WWP structures, are expected to behave like a re-naturalized bank system which can increase the abundance of rheophilic fish species (Ramler and Keckeis, 2019).

The influence of flow conditions and the water depth difference Δy upstream and downstream of the series of structures (or of the single structure in case of isolated WWPs) on the determination of the morphological features has been extensively shown in literature (e.g., Pagliara et al., 2015;

Palermo et al., 2021; Roy et al., 2021). Such dependence is further corroborated by the present study (Figure 14). Namely, the relative drop in the water surface level up- and down-stream of the WWP (or of the series of structures) $\Delta y/h_{tw}$ resulted to be a key parameter affecting the transition between the two morphology types *NS* and *S*. On the contrary, the number of structures *n* had little influence on the scour morphology types classifications. In a similar fashion, the presence of vegetation and the structure submergence also resulted to be non-influential in such classification. The different morphology types were distinguished and classified by plotting experimental values of $\Delta y/h_{tw}$ as function of F_{deq} (Figure 14a) and F_{vdeq} (Figure 14b). The identification of the scour morphology type is of paramount importance for a correct design of WWPs, mainly to identify portions of the channel banks potentially undergoing excessive erosion.

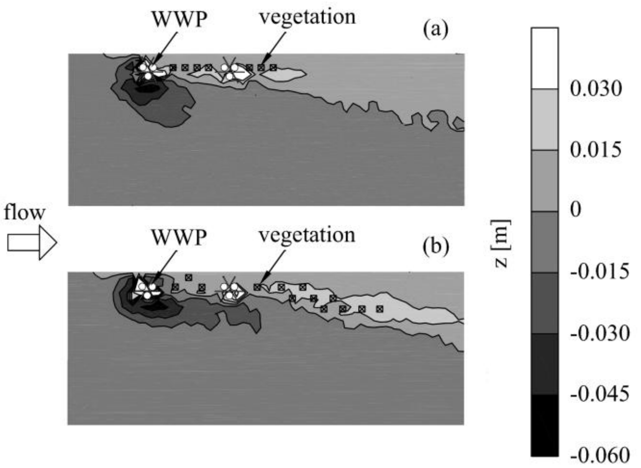

Fig. 15. Contour map showing equilibrium scour morphology in case of two WWPs in series configuration in presence of a) symmetric vegetation (test 20) and b) staggered vegetation (test 25).

Finally, Figure 15 presents the equilibrium scour morphology for two A_3 phase tests (test 20 and 25), both having n = 2, to compare the effect of symmetric and staggered vegetation arrangement on the overall scour morphology. In Figure 15a (test 20), the two WWPs in series configuration is accompanied by a symmetric vegetation growth and the scour hole is mainly occurring at the first WWP structure in the series along with extended wing-like dune formation in between the two WWP and in the downstream basin. On increasing both the tailwater and discharge in Figure 15b (test 25) with staggered vegetation growth, both the dune and scour region become more pronounced, and the length of scour and dune increases with higher number of vegetation elements (n_v) as corroborated in Fig. 9b. This is because higher number of vegetation elements pose multiple flow obstacles which instigates sequential local erosions at the base of the vegetation elements resulting in longitudinal expansion of the scour hole as well as the dune formation. However, vegetation pattern (symmetric or staggered) does not impact the equilibrium scour morphology significantly.

4 CONCLUSION

Experimental tests were conducted in a straight channel under clear water condition with Worked Wood Piles (WWP), i.e., low-head river restoration structures made of large wood logs, by varying the flow discharge, the tailwater depth, and the number of structures placed in a series arrangement. Furthermore, the natural growth of vegetation was also simulated by using two different types of vegetation elements, characterized by different heights.

We systematically varied hydraulic and geometrical conditions and derived empirical equations to predict the maximum scour depth and dune height, as well as the maximum scour length.

Results showed that in-stream vegetation has negligible impact on the maximum scour depth and dune height due to isolated WWP or multiple WWPs in series under clear water condition for the tested range of parameters. Conversely, height and number of vegetation have a considerable impact on maximum scour length. Particularly, greater number of in-stream vegetation elements results in higher scour and dune length.

The temporal evolution and the equilibrium configuration were also investigated. The equilibrium configuration is characterized by a distinct scour region in the vicinity of the structure, while a dune forms in the downstream stilling basin in a wing-like formation. Such morphological features introduce significant variations in flow and water depth in the channel which have a positive impact on fluvial biodiversity. Particularly, deep scour potholes provide lower temperatures coupled with possible flow exchange with hyporheic zone, thereby, creating a sanctuary for various aquatic organisms. Moreover, for a series arrangement of 2 or 3 WWPs, the scour and dune formations become more pronounced and elongated. A similar trend is evidenced for increasing inflow discharge and tailwater depth, for otherwise similar conditions. Two morphology types and the correspondent existence fields were identified: (i) the type *NS* presents no scour formation downstream of the first WWP, and a marked dune formation connected to the downstream end of the first WWP, enhancing bank protection; (ii) the type *S* shows deep scour all around the first WWP, and a dune formation shifted downstream compared to the *NS*-type, thus potentially resulting in excessive bank erosion and subsequent failure. The scour morphology classification is essential for a safe design of WWPs, e.g., to identify sites for dredge disposal and aquatic species refuge, and areas of the channel bank prone to excessive erosion. In general, the scour-dune pattern in vicinity of WWP structures both in presence and absence of vegetation serve as a re-naturalized bank more suitable for habitation compared to traditional riprap banks. As for the temporal evolution, the rate of expansion of the scour and dune regions for isolated WWP is uniform in time, while it is significantly affected by the inflow conditions in case of a series configuration.

Overall, the scour characteristics at WWPs have been examined in the presence of in-stream vegetation at various stages of growth which demonstrates the potential of such structures to emerge as an effective eco-friendly river restoration technique. However, future studies should investigate the scour characteristics due to WWPs in vegetated channels under live bed condition. Also, the flow characteristics and turbulent structures across low-head LW based structures in conjugation with in-stream vegetation is an important future topic of study.

NOTATION

A_0 – reference test without presence of vegetation (duration = 4 hours)
A_i – i-th phase of the scour process, with i an integer ranging between 1 and 3.
B – channel width

b – blockage width of an individual WWP in the direction perpendicular to the flow
d – distance of separation between two consecutive WWP in series arrangement
d_{50} – mean particle diameter
f – functional symbol
F_{d50} – densimetric Froude number
F_{deq} – equivalent densimetric Froude number
F_{vdeq} – equivalent densimetric Froude number applicable for vegetated channels
g – gravitational acceleration
h_{st} – height of the structure
h_{tw} – tailwater depth
h_v – height of vegetation element
LW – Large Wood
l_p – length of the wooden member
l_m – maximum scour length
l_M – maximum dune length
n – number of structures (in series arrangement)
n_v – number of vegetation elements
NS – "No Scour" morphology type
Q – discharge
s – distance of the first WWP from the channel entrance
S – "Scour" morphology type
t – time from the start of experiment
t_i – duration of the phase A_i with i an integer ranging between 1 and 3
t_t – overall duration of the three phases, i.e., A_1, A_2 and A_3
T – reference time
U – mean flow velocity
U_c – critical velocity
V_l – low height shrub vegetation element
V_h – high leafy vegetation element
WWP – worked wood piles
z_m – maximum scour depth
z_M – maximum dune height
Δy – difference between water surface levels upstream and downstream of the structure(s)
$\Delta\rho$ – reduced sediment density
φ – characteristic length of scour/dune geometry
Φ – non-dimensional characteristic length of scour/dune geometry
ρ – water density
ρ_s – sediment density
σ – sediment non-uniformity parameter

REFERENCES

Barenblatt, G.I., 1987. Dimensional analysis. Gordon and Breach Science Publishers, New York, ISBN 3-7186-0438-8.

Bayley, P.B., 1991. The flood pulse advantage and the restoration of river-floodplain systems. Regul. River. Res. Manag., 6, 75–86. DOI: 10.1002/rrr.3450060203

Bhuiyan, F., Hey, R.D., Wormleaton, P.R., 2010. Bank-attached vanes for bank erosion control and restoration of river meanders. J. Hydraul. Eng., 136, 583–596. DOI: 10.1061/(ASCE)HY.1943-7900.0000217

Bombardelli, F.A., Palermo, M., Pagliara, S., 2018. Temporal evolution of jet induced scour depth in cohesionless granular beds and the phenomenological theory of turbulence. Phys. Fluids, 30, 1–19. DOI: 10.1063/1.5041800

Bormann, E., Julien, P.Y., 1991. Scour downstream of grade control structures. J. Hydraul. Eng., 117, 579–594. DOI:10.1061/(ASCE)0733-9429(1991)117:5(579)

Breusers, H.N.C., Raudkivi, A.J., 1991. Scouring: hydraulic structures design manual Series. Balkema, The Netherlands.

D'Agostino, V., Ferro, V., 2004. Scour on alluvial bed downstream of grade-control structures. J. Hydraul. Eng., 130, 1–14. DOI:10.1061/(ASCE)0733-9429(2004)130:1(24)

Dey, S., Raikar, R.V., 2005. Scour in long contractions. J. Hydraul. Eng., 131, 1036–1049. DOI: 10.1061/(ASCE)0733-9429(2005)131:12(1036)

Dey, S., Sarkar, A., 2006. Scour downstream of an apron due to submerged horizontal jets. J. Hydraul. Eng., 132, 246–257. DOI: 10.1061/(ASCE)0733-9429(2006)132:3(246)

Dey, S., Sarkar, A. (2008). Characteristics of submerged jets in evolving scour hole downstream of an apron. Journal of Engineering Mechanics, 134, (11), 927–936.

Di Nardi, J., Palermo, M., Bombardelli, F.A., Pagliara, S., 2021. The phenomenological theory of turbulence and the scour evolution downstream of grade-control structures under steady discharges. Water, 13, 2359. DOI: 10.3390/w13172359

Di Nardi, J., Palermo, M., Bombardelli, F.A., Pagliara, S., 2022. First principles-based approach for 3D scour processes under variable jet discharge. Water Resour. Res., 58, e2021WR030346. DOI: 10.1029/2021WR030346

Fischenich, J.C., Morrow, J.V. Jr., 2000. Streambank habitat enhancement with large woody debris (Report No. ERDC TN-EMRRP-SR-13). Army Engineer Waterways Experiment Station Vicksburg MS Engineer Research and Development Center.

Gippel, C.J., 1995. Environmental hydraulics of large woody debris in streams and rivers. J. Env. Eng., 121, 388–395. DOI: 10.1061/(ASCE)0733-9372(1995)121:5(388)

Heller, V., 2011. Scale effects in physical hydraulic engineering models. J. Hydraul. Res., 49, 293–306. DOI: 10.1080/00221686.2011.578914.

Hoffmans, G.J.C.M., 1998. Jet scour in equilibrium phase. J. Hydraul. Eng., 124, 430–437. DOI: 10.1061/(ASCE)0733-9429(1998)124:4(430)

Hoffmans, G.J.C.M., Verheij, H.J., 1997. Scour manual. Balkema, The Netherlands.

Jahadi, M., Afzalimehr, H., Rowinski, P.M., 2019. Flow structure within a vegetation patch in a gravel-bed river. J. Hydrol. Hydromech., 67, 154–162. DOI: 10.2478/johh-2019-0001

Kałuża, T., Radecki-Pawlik, A., Szoszkiewicz, K., Plesiński, K., Radecki-Pawlik, B., Laks, I., 2018. Plant basket hydraulic structures (PBHS) as a new river restoration measure. Sci. Total. Environ., 627, 245–255. DOI: 10.1016/j.scitotenv.2018.01.029.

Keller, E.A., Swanson, F.J., 1979. Effects of large organic material on channel form and fluvial processes. Earth. Surf. Proc., 4, 361–380. DOI: 10.1002/esp.3290040406

Kurdistani, S.M., Pagliara, S., Palermo, M., 2023. Analysis of fish migration in correspondence with wood and rock-made instream structures. Geomorphology, 439, 108836. DOI: 10.1016/j.geomorph.2023.108836.

Maryland Department of the Environment Water Management Administration, 2000. Channel stabilization and rehabilitation techniques, Maryland's guidelines to waterway construction.

Melville, B.W., Chiew, Y.M., 1999. Time scale for local scour at bridge piers. J. Hydraul. Eng., 125, 59–65. DOI: 10.1061/(ASCE)0733-9429(1999)125:1(59).

Neill, C.R., 1968. Note on initial movement of coarse uniform bed-material. J. Hydraul. Res., 6, 173–176. DOI: 10.1080/00221686809500228

Neuhaus, V., Mende, M., 2021. Engineered Large Wood Structures in stream restoration projects in Switzerland: practice-based experiences. Water, 13, 2520. DOI: 10.3390/w13182520

Odgaard, A.J., Mosconi, C.E., 1987. Stream bank protection by submerged vanes. J. Hydraul. Eng., 113, 520–536. DOI: 10.1061/(ASCE)0733-9429(1987)113:4(520)

Odgaard, A.J., Spoljaric, A., 1986. Sediment control by submerged vanes. J. Hydraul. Eng., 112, 1164–1181. DOI: 10.1061/(ASCE)0733-9429(1986)112:12(1164)

Oliveto, G., Hager, W.H., 2002. Temporal evolution of clear-water pier and abutment scour. J. Hydraul. Eng., 128, 811–820. DOI: 10.1061/(ASCE)0733-9429(2002)128:9(811)

Pagliara, S., Kurdistani, S.M., 2016. Flume experiments on scour downstream of wood stream restoration structures. Geomorphology, 279, 141–149. DOI: 10.1016/j.geomorph.2016.10.013

Pagliara, S., Das, R., Palermo, M., 2008. Energy dissipation on submerged block ramps. J. Irrig. Drain. Eng., 134, 527–532. DOI: 10.1061/(ASCE)0733-9437(2008)134:4(527)

Pagliara, S., Hassanabadi, L., Kurdistani, S.M., 2015. Clear water scour downstream of log deflectors in horizontal channels. J. Irrig. Drain. Eng., 141, 1–8, 04015007. DOI: 10.1061/(ASCE)IR.1943-4774.0000869

Pagliara, S., Hager, W.H., Minor, H.E., 2006. Hydraulics of Plane Plunge Pool Scour. J. Hydraul. Eng., 132, 450–461. DOI:10.1061/(ASCE)0733-9429(2006)132:5(450).

Pagliara, S., Palermo, M., Roy, D., 2020a. Scour around double-winged log frames under clear water condition. J. Irrig. Drain. Eng., 146, 04020038. DOI: 10.1061/(ASCE)IR.1943-4774.0001517

Pagliara, S., Palermo, M., Roy, D., 2020b. Experimental investigation of erosion processes downstream of block ramps in mild curved channels. Environ. Fluid. Mech., 20, 339–356. DOI: 10.1007/s10652-019-09681-1

Pagliara, S., Radecki-Pawlik, A., Palermo, M., Plesiński, K., 2017. Block ramps in curved rivers: morphology analysis and prototype data supported design criteria for mild bed slopes. River. Res. Appl., 33, 427–437. DOI: 10.1002/rra.3083

Pagliara, S., Roy, D., Palermo, M., 2021. Scour features at wood bundles. Water, 13, 2118. DOI: 10.3390/w13152118

Palermo, M., Pagliara, S., Bombardelli, F.A., 2020. Theoretical approach for shear-stress estimation at 2D equilibrium scour holes in granular material due to subvertical plunging jets. J. Hydraul. Eng., 146, 1–12. DOI: 10.1061/(ASCE)HY.1943-7900.0001703

Palermo, M., Roy, D., Pagliara, S., 2021. Morphological characteristics of eco-friendly protected basins downstream of block ramps in river bends. Geomorphology, 377, 107587. DOI: 10.1016/j.geomorph.2020.107587

Ramler, D., Keckeis, H., 2019. Effects of large-river restoration measures on ecological fish guilds and focal species of conservation in a large European river (Danube, Austria). Sci. Total. Environ., 686, 1076–1089. DOI: 10.1016/j.scitotenv.2019.05.373

Roy, D., Pagliara, S., 2022a. Preliminary Analysis of the Effect of Worked Wood Piles in Straight Channels. In: Proceedings of the ISHS 2022 9th International Symposium on Hydraulic Structures. IAHR, Roorkee, India. DOI: 10.26077/34f4-8489

Roy, D., Pagliara, S., 2022b. Equilibrium morphology and scour evolution at blunt nosed chevrons. River. Res. Appl., 38, 499–512. DOI: 10.1002/rra.3911

Roy, D., Pagliara, S., Palermo, M., 2021. Experimental analysis of scour features at chevrons in straight channel. Water, 13, 971. DOI: 10.3390/w13070971

Schalko, I., Schmocker, L., Weitbrecht, V., Boes, R.M., 2018. Backwater rise due to large wood accumulations. J. Hydraul. Eng., 144, 04018056. DOI: 10.1061/(ASCE)HY.1943-7900.0001501

Schalko, I., Schmocker, L., Weitbrecht, V., Boes, R.M., 2020. Laboratory study on wood accumulation probability at bridge piers. J. Hydraul. Eng., 58, 566–581. DOI: 10.1080/00221686.2019.1625820

Scurlock, S.M., Cox, A.L., Thornton, C.I., Baird, D.C., 2012a. Maximum velocity effects from vane-dike installations in channel bends. In: Proceedings of World Environmental and Water Resources Congress 2012. ASCE, Albuquerque, USA. DOI: 10.1061/9780784412312.261

Scurlock, S.M., Thornton, C.I., Abt, S.R., 2012b. Equilibrium scour downstream of three-dimensional grade-control structures. J. Hydraul. Eng., 138, 167–176. DOI: 10.1061/(ASCE)HY.1943-7900.0000493

Stoffers, T., Buijse, A.D., Geerling, G.W., Jans, L.H., Schoor, M.M., Poos, J.J., Verreth, J.A.J., Nagelkerke, L.A.J., 2022. Freshwater fish biodiversity restoration in floodplain rivers requires connectivity and habitat heterogeneity at multiple spatial scales. Sci. Total. Environ., 838, 156509. DOI: 10.1016/j.scitotenv.2022.156509.

Wilkerson, G., Sharma, S., Sapkota, D., 2019. Length for uniform flow development in a rough laboratory flume. J. Hydraul. Eng., 145, 06018018. DOI: 10.1061/(ASCE)HY.1943-7900.0001554.

Received 1 November 2024
Accepted 14 March 2025

Appendices

Table 1. Summary of experimental results.

Test	**Test phase**	Q	h_{tw}	Δy	n	n_v	h_v	z_m	l_m	z_M	l_M	U/U_c
(–)	(–)	(m³/s)	(m)	(m)	(–)	(–)	(m)	(m)	(m)	(m)	(m)	(–)
1	A_1	0.011	0.075	0.004	1	–	–	0.051	0.400	0.021	1.040	0.84
2	A_2	0.011	0.075	0.004	1	31	0.045	0.053	0.780	0.025	1.420	0.84
3	A_3	0.011	0.075	0.004	1	31	0.090	0.053	0.900	0.025	2.040	0.84
4	A_0	0.011	0.075	0.003	1	–	–	0.051	0.700	0.019	1.470	0.84
5	A_0	0.008	0.056	0.003	1	–	–	0.054	0.600	0.022	1.070	0.85
6	A_1	0.008	0.056	0.003	1	–	–	0.051	0.320	0.019	0.640	0.82
7	A_2	0.008	0.056	0.003	1	12	0.045	0.055	0.680	0.025	0.890	0.82
8	A_3	0.008	0.056	0.003	1	12	0.090	0.055	0.690	0.025	1.170	0.82
9	A_1	0.014	0.094	0.003	1	–	–	0.052	0.200	0.019	0.430	0.79
10	A_2	0.014	0.094	0.003	1	8	0.045	0.052	0.280	0.017	0.710	0.79
11	A_3	0.014	0.094	0.003	1	8	0.090	0.052	0.500	0.017	0.800	0.79
12	A_0	0.005	0.036	0.002	1	–	–	0.051	0.590	0.019	1.310	0.86
13	A_1	0.005	0.036	0.002	1	–	–	0.046	0.270	0.017	0.730	0.86
14	A_1	0.005	0.036	0.004	2	–	–	0.041	0.450	0.019	0.940	0.86
15	A_2	0.005	0.036	0.004	2	10	0.045	0.041	0.670	0.015	1.400	0.86
16	A_3	0.005	0.036	0.004	2	10	0.090	0.042	0.780	0.014	1.710	0.86
17	A_0	0.005	0.036	0.003	2	–	–	0.042	0.640	0.019	1.100	0.86
18	A_1	0.008	0.056	0.004	2	–	–	0.044	0.500	0.021	0.830	0.82
19	A_2	0.008	0.056	0.003	2	7	0.045	0.044	0.560	0.022	1.100	0.82
20	A_3	0.008	0.056	0.005	2	7	0.090	0.052	0.570	0.020	1.330	0.82
21	A_0	0.008	0.056	0.005	2	–	–	0.050	0.710	0.024	1.400	0.82
22	A_0	0.011	0.075	0.005	2	–	–	0.044	0.760	0.021	1.210	0.81

23	A_1	0.011	0.075	0.005	2	–	–	0.045	0.380	0.025	0.990	0.81
24	A_2	0.011	0.075	0.005	2	13	0.045	0.048	0.610	0.025	1.230	0.81
25	A_3	0.011	0.075	0.005	2	13	0.090	0.050	0.690	0.025	1.580	0.81
26	A_0	0.014	0.094	0.004	2	–	–	0.053	0.680	0.025	1.070	0.79
27	A_1	0.014	0.094	0.004	2	–	–	0.052	0.390	0.023	0.890	0.79
28	A_2	0.014	0.094	0.004	2	17	0.045	0.052	0.590	0.030	1.040	0.79
29	A_3	0.014	0.094	0.005	2	17	0.090	0.052	0.740	0.030	1.380	0.79
30	A_0	0.005	0.036	0.003	3	–	–	0.042	0.450	0.014	1.620	0.86
31	A_1	0.005	0.036	0.003	3	–	–	0.036	0.450	0.014	1.580	0.86
32	A_2	0.005	0.036	0.004	3	12	0.045	0.036	0.730	0.013	1.650	0.86
33	A_0	0.008	0.056	0.004	3	–	–	0.045	0.650	0.015	1.640	0.82
34	A_1	0.008	0.056	0.004	3	–	–	0.041	0.130	0.018	1.500	0.82
35	A_2	0.008	0.056	0.004	3	9	0.045	0.041	0.660	0.018	1.650	0.82
36	A_3	0.008	0.056	0.004	3	9	0.090	0.041	0.760	0.017	1.640	0.82
37	A_0	0.011	0.075	0.005	3	–	–	0.044	0.790	0.020	1.640	0.81
38	A_1	0.011	0.075	0.005	3	–	–	0.043	0.220	0.024	1.430	0.81
39	A_2	0.011	0.075	0.005	3	10	0.045	0.042	0.560	0.025	1.650	0.81
40	A_3	0.011	0.075	0.004	3	10	0.090	0.043	0.650	0.025	1.650	0.81
41	A_0	0.014	0.094	0.004	3	–	–	0.044	0.800	0.020	1.620	0.79
42	A_1	0.014	0.094	0.005	3	–	–	0.044	0.450	0.020	1.320	0.79
43	A_2	0.014	0.094	0.005	3	10	0.045	0.044	0.530	0.019	1.510	0.79
44`	A_3	0.014	0.094	0.005	3	10	0.090	0.043	0.700	0.021	1.670	0.79